PINPOINTING THE TIMING OF WEAK LAYER FAILURE: A CASE STUDY OF A LARGE, WIDESPREAD NATURAL AVALANCHE CYCLE IN THE BITTERROOT MOUNTAINS INTERNATIONAL SNOW SCIENCE WORKSHOP 2026, WHISTLER, CANADA

James Peabody*, Nathalie de Leeuw, and Ben VandenBos

West Central Montana Avalanche Center, Missoula, MT, USA

ABSTRACT: In March 2026, a multi-day storm deposited over 180 mm of snow water equivalent (SWE) across the Bitterroot Mountains of Montana and Idaho. Prior to the storm, the snowpack contained multiple buried persistent weak layers, including a crust/facet layer, referred to as the January Drought Layer (JDL). In the days and weeks before the storm, cornice fall triggered large avalanches on the JDL, and forecasters anticipated a widespread natural cycle during the storm. A key forecasting challenge with persistent slab problems is predicting at what point during a storm cycle natural avalanches are most likely to occur. Previous studies have linked weather station data to persistent slab avalanche occurrence, however without knowledge of exactly when during the storm the avalanche released, it is difficult to determine exactly how much new load it took for avalanches to occur. The Bitterroot forecast zone receives few user observations, and it is unlikely observers would have been reporting the timing of avalanche occurrence during the storm. To estimate the timing of release within the storm, we measured SWE above the JDL at both the crown face and on the bed surface of a persistent slab avalanche that released during the storm. By correlating these measurements to continuous SWE data from a SNOTEL station approximately 6.5 km away, we are able to determine approximately when, and after how much load the avalanche occurred. We also used photos and mapping software to collect slope angle and aspect data from 23 additional avalanches within a 13 km radius that occurred during the same cycle. We can use this geospatial data to determine if these avalanches were similar in aspect and elevation to the avalanche where we collected the measurements. This data will allow us to look for patterns in avalanche release from this storm and determine if loading amounts before triggering may have been similar. This method has potential to improve forecasting of persistent slab cycles in intermountain snowpacks.

KEYWORDS: Timing of weak layer failure; avalanche forecasting; geospatial analysis; deep slab instability; case study

1. INTRODUCTION

Forecasting the timing of natural avalanche cycles is notoriously difficult, especially when dealing with persistent weak layers. Large avalanche forecasting programs have access to many points of data such as satellite detection, webcams, sensors, and guiding operations in their forecast area. With these resources, accuracy of timing can be more precise. Smaller public centers do not always have the benefit of a community like this and must rely on data with higher levels of uncertainty, such as weather data and snowpack data, rather than avalanche occurrence data (LaChapelle, 1980). In the spring of 2026 with a known weak layer in the forecast area and a large storm on the horizon, the West Central Montana Avalanche Center (WCMAC) wondered when this long-developed weak layer would reach its tipping point. Schauer et al. (2024) provided a key guideline for predicting weak-layer failure, finding that "precipitation loading events only produced avalanches when the total cumulative SWE above the crust was between 9.1–40.6 cm (3.6″–16″) since the crust had formed. Once there was greater than 40.6 cm (16″) of cumulative SWE above the crust, we did not observe any activity attributed to precipitation loading as the primary driver of instability…" but did not offer much guidance on specific thresholds relevant to our snowpack. The goal of this case study was to "hindcast" the incoming avalanche cycle using accessible tools such as SNOTEL data, snowpack models, and snow density kits to help pinpoint timing during the storm and better understand the thresholds of weak-layer overloading. Using photography, georeferencing, and geospatial analysis, we were also able to map avalanche crowns and look for patterns in aspect, elevation, and distribution. These tools are affordable, accessible, and simple to work with. Our goal is to use the data we collected from this storm in 2026,

* *Corresponding author address:*
Jack Peabody, WCMAC
PO Box 72, Missoula, MT 59806.
tel: +1 509-509-0864
email: jack@peabodyfamily.org

https://doi.org/10.15788/1790099067

to help us better predict thresholds for weak layer failure in similar storm events in the future.

1.1 Study area

The WCMAC forecasts for three separate zones. This study focuses on the southernmost zone, known as the Bitterroot Zone. The Bitterroot Mountains span approximately 160 km (100 miles) along the Idaho–Montana border. Access is limited by long approaches through Wilderness in much of the range. This case study focuses on the central portion of the range, where motorized access to near the range crest is possible.

The Bitterroot Mountains are characterized by a long series of east-west trending ridges and U-shaped valleys that gradually climb towards a long crest. Storms approaching from the west are funneled toward the Bitterroots. The first high peaks they encounter are those of the Bitterroot Crest, with elevations ranging 2,440–2,740 m (8,000–9,000 ft), with tree line around 3,000 m (7,500 ft). The snow climate along the crest is intermountain (Mock and Birkeland, 2000). The study area, comprising the Lost Horse, Bear, and Spruce Creek drainages, is referred to herein as the Lost Horse study area.

1.2 Meteorological instrumentation

The Twin Lakes SNOTEL site, located at the center of the study area, is approximately 1 km (0.6 mi) west of the Bitterroot Crest, situated at 1,950 m (6,400 ft) on an ENE aspect surrounded by dense forest canopy, with average winter daily highs near freezing and median annual precipitation of 1.65 m (65.1 in) (NRCS, 2026).

1.3 Snowpack history

During January, the study area experienced a 15-day period with no measurable precipitation, punctuated by periods of above-freezing temperatures. This period ended on January 26th, and the resulting layer of crusts and facets was named the January Drought Layer (JDL). A version of this layer existed everywhere in the forecast area, on all aspects and elevations that had snow cover in January. In areas protected from scouring winds and solar radiation, the JDL was more prevalent. Over the coming weeks this layer was gradually buried by a series of minor storms, within the “Active Cumulative Precipitation” limits defined in Schauer et al. (2024). The largest storm deposition to follow occurred on February 24th/25th, depositing approximately 5 cm (2 in) of SWE in the study area. Following the storm the first natural avalanches on this JDL layer were reported. These avalanches were along the Bitterroot Crest, triggered by cornice fall. The forecasting team was surprised by the large crown lengths, as there had been no reported avalanches on this layer prior to this storm.

1.4 Forecast

The West Central Montana Avalanche Center (WCMAC) is a Type 2 Center, meaning it forecasts on a partial, rather than daily (7-day), schedule, with a small user group. Most of the observations used by the center are generated by the staff. Public observations are infrequent. With a small team, a known weak layer, and a large storm incoming, the team employed threshold-based forecasting methods, but found little existing research on the subject.

When the storm began on March 11th, the forecasted water amounts shifted to favor the Central Bitterroot, the same location where the cornice-fall avalanches had occurred. Given that the storm event is a region wide, multiday atmospheric river system the forecast team had uncertainty about the size and distribution of these potential avalanches, and elected to issue avalanche warnings on March 12th, 13th and 14th. With the storm playing out over days and a lack of visibility, uncertainty existed about the timing of avalanche occurrence.

2. METHODS

This study was developed from photography and snowpack data collected in the field. Therefore there are two paths of data collected, one being snow measurements, and the other being photos that were georeferenced for avalanche crown data.

2.1 Snowpack sampling

Following Ben's initial trip into Lost Horse, WCMAC forecast staff returned to make direct observations of one of the crowns on March 18th. Comparison of snow deposition on adjacent crowns in the study area indicates there were minimal differences in timing between avalanche crowns. This site was less wind-affected than most of the other crown locations and was selected since it was more likely the snowpack aligned to the basin's SNOTEL site, which was non-wind affected. The crown wall study site was approximately 6.5 km (4 mi) and 370 m (1,200 ft) higher than the SNOTEL site.

Once at site, the crown was cleaned, bed surface identified, and 20 cm (8 in) increments were measured out. Using a 30 cm (12 in) snow sample tube, hanging spring scale, and a metal crystal card, the crown wall was sampled every 20 cm (8 in) to measure SWE and calculate density. These values were recorded, and the additional snow that had fallen since the major storm on the bed surface was also measured for height and SWE.

We subtracted the amount of new snow on the bed surface from the total crown height, in order to infer crown height at the time the avalanche occurred.

This load was then expressed as a percentage of the crown's total accumulation since the JDL was buried, and that same percentage was applied to the Twin Lakes SNOTEL SWE record over the same period (JDL burial through final field measurement). This proportional method assumes the crown site and the SNOTEL site accumulated SWE at roughly the same relative rate over the season, an assumption we felt was reasonable given the broad, multi-day nature of the storms involved. Applying this percentage to the SNOTEL record allowed us to identify the specific date, and using hourly SNOTEL data, the approximate time, at which the layer would have reached its failure load.

This same method was also applied to infer the load carried by the layer before the storm began versus the load added during the storm itself, in order to evaluate how much of the failure load had already accumulated prior to the triggering storm.

Following this, individual loading events prior to the avalanche were also identified within the SNOTEL SWE record. Each event's magnitude was then expressed as a percentage of the total load carried by the layer at failure, rather than by magnitude alone, per methods in Schauer et al. (2024). This allowed for evaluation of whether any single loading event, including the final triggering storm, stood out as disproportionately significant, or whether failure was better explained by cumulative loading across many smaller events over time.

2.2 Crown comparisons

On March 16th, one forecaster, Ben VandenBos, traveled to the central Bitterroot to survey the damage. Many of Ben's photos were taken from a high point near the end of the Lost Horse Creek drainage, known as Forecaster Summit. Forecaster Summit is approximately 4.0 km (2.5km) southeast from the Twin Lakes SNOTEL site. Using Ben's photos of crowns, Caltopo lines were created to analyze the aspect and elevation profiles of each crown to see if there was any aspect or slope angle dependence to where avalanches occurred, and therefore where the weak layer was most likely to share characteristics. Digital mapping of the observed avalanche activity yielded 24 crowns totaling 9,866 linear metes (32,370 ft).

Forecaster Summit was well situated to look at dozens of ridges, sub ridges, and peaks within 10 km (6.2 mi). Knowing his coordinates and time of day, mapping the crowns required comparison of 3D imagery to locate the ridge, and subsequently map the crown on that terrain feature.

Once the crowns were mapped, crowns were digitally sampled in 7.6 m (25 ft) intervals for aspect and elevation data. This short sampling distance was selected based on the highly variable topography. These points were grouped by avalanche and used in the data analysis for elevation and aspect occurrence. Using the same sample interval for all avalanche crowns also allows for calculations to be both weighted and unweighted for analysis.

Aspect data was analyzed using circular statistics to account for the wraparound nature of compass direction. A circular mean and resultant vector length (R) were calculated both on an unweighted, per-avalanche basis and on a mass-weighted, per-point basis, where R is a measure of directional concentration ranging from 0 (aspects scattered evenly in all directions) to 1 (all aspects identical). Individual sample points were used so that points from larger avalanches contributed more to the final result.

Elevation data was similarly analyzed both on an unweighted, per-crown basis and a mass-weighted, per-point basis, binned into 76 m (250 ft) increments, to evaluate whether avalanche mass was evenly distributed across the sampled elevation range or concentrated within a narrower band.

3. RESULTS

3.1 Timing

The total crown wall of our study avalanche had a SWE of 46.1 cm (18.1 in). New snow on the bed surface totaled a SWE of 5.97 cm (2.35 in). Subtracting the bed surface SWE from the crown wall SWE isolated the load that was present on the JDL layer at the moment of failure, resulting in 40.13 cm (15.80 in) SWE.

During this same period SNOTEL SWE increased by 38.9 cm (15.31 in). Before the storm, The SNOTEL was at 70.6 cm (27.8 in) of SWE. This implies the avalanche likely occurred when the SNOTEL site was around 88.19 cm (34.72 in). Cross-referencing this target value with the hourly SWE data suggests the avalanche occurred on March 14th between 1:00 AM (88.14 cm / 34.7 in) and 2:00 AM (88.39 cm / 34.8 in). This estimate aligns with the field observations, avalanche warnings, and avalanche observations in the surrounding regions. The accuracy/precision of this is limited by the assumption that the SWE accumulation rate at the crown wall is consistent with the accumulation rate at the SNOTEL station, despite the 6.5 km (4 mi) separation and 370 m (1,200 ft) elevation difference. Given that the storm event is a region wide, multiday atmospheric river system, we believe this assumption is reasonable (Figure 2).

3.2 Loading events

Following Schauer et al.'s (2024) suggestion that individual loading events may be more informative expressed as a percentage of total load above the crust rather than in absolute magnitude, we segmented the SNOTEL SWE record from JDL burial (Jan 26) through the estimated avalanche failure time (1–2 AM Mar 14) into discrete loading events, identified as periods of sustained SWE increase separated by flat or declining (settlement) periods.

Seven discrete loading events were identified over the 47-day period the JDL was buried prior to failure. No single event prior to the storm exceeded 17% of the total load the layer was supporting until failure. The largest of the previous six snowfall events (Feb 20th–28th) corresponds to the first natural avalanches observed on the JDL layer, described in the introduction as having occurred during a storm at the end of February and having surprised the forecasting team with their crown lengths. These avalanches were not observed in motion, but they were first noted in the field on February 28th, with their timing estimated at February 24th/25th. The SNOTEL record shows that within the Feb 20–28th loading event, 53.7% of the storm load (3.55 of 6.61 cm / 1.40 of 2.60 in) was deposited in a single day, February 25th, which is consistent with that field-based estimate.

3.3 Aspect distribution

The unweighted circular mean aspect, treating each of the 24 avalanches equally regardless of size, was 47.6° (true NE), with a resultant vector length (R) of 0.882.

When weighted by crown mass, the mean aspect shifted to 54.6° (NE bordering on ENE), with R increasing to 0.920. As seen in Figure 1, the higher R in the weighted analysis indicates the largest avalanches were on more NE slopes, while the two aspect outliers (both NW-facing) pulled the unweighted average further off-axis than they did the weighted average, since they represent a small fraction of total mass. An R value above 0.9 in the mass-weighted analysis reflects an unusually strong directional signal for a natural process and quantitatively supports wind loading out of the SW as the dominant control on avalanche aspect during this storm.

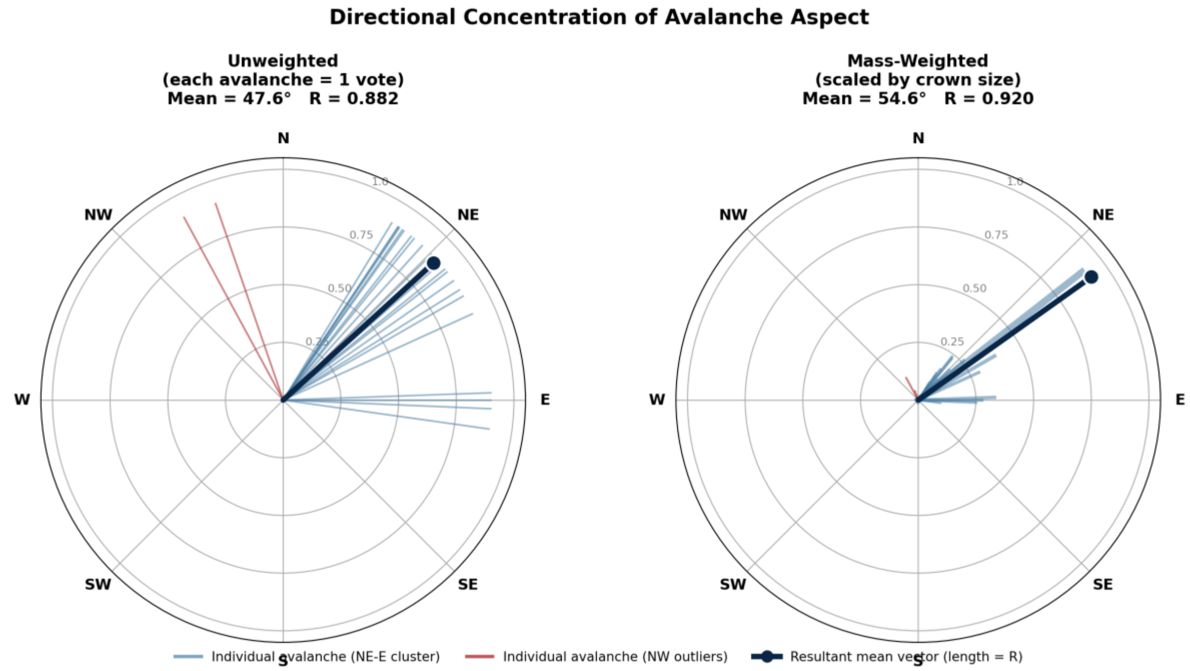

Figure 1: Directional concentration of avalanche aspect, unweighted (per avalanche) and mass-weighted (per sampled point). Each line represents one avalanche's aspect, colored by cluster (blue = NE–E cluster, red = NW outliers); the bold arrow shows the resultant mean vector, with length equal to R.

3.4 Elevation distribution

Avalanche crown elevations were similarly analyzed both by simple average across avalanches and weighted by sampled mass. The unweighted mean elevation across all 24 avalanches was 2,283 m (7,491 ft); the mass-weighted mean was nearly identical at 2,288 m (7,508 ft), indicating that crown size was not strongly elevation-dependent. Combining the two central bands (2,210–2,286 m and 2,286–2,362 m / 7,250-7,500 ft and 7,500-7,750 ft), 54.2% of avalanches (by count) and 62.4% of total avalanche mass (mass-weighted) occurred in this range despite this representing less than half of the full sampled elevation range (2,072–2,516 m / 6,798–8,253 ft). Notably, activity dropped off sharply above 2,438 m (8,000 ft), with only a single, small-mass avalanche (1.4% of total weight) occurring in the highest 76 m (250 ft) band, even though ridgelines in the study area extend to roughly 2,500 m (8,400 ft).

4. DISCUSSION

4.1 Timing reconstruction

This SWE proportionality method places the avalanche occurrence of the sampled crown in the early morning of March 14th. In Figure 2, one can note the large SWE increase during the storm that overloaded the JDL. The timing of this avalanche indicates the avalanche cycle was at the tail end of the event after a majority of loading had already occurred. When comparing the pre storm vs. storm load percentages, the storm added 45% of the total load for failure. This number shows the layer was already carrying a majority of the load (55%) before failure, illustrating the storm pushed an already loaded weak layer over the edge into a deep slab cycle. This timing is consistent with the forecaster's hypothesis of avalanche occurrence and subsequent issuing of an avalanche warning on March 12th, 13th and 14th, and provides validity to the decision making for this storm event.

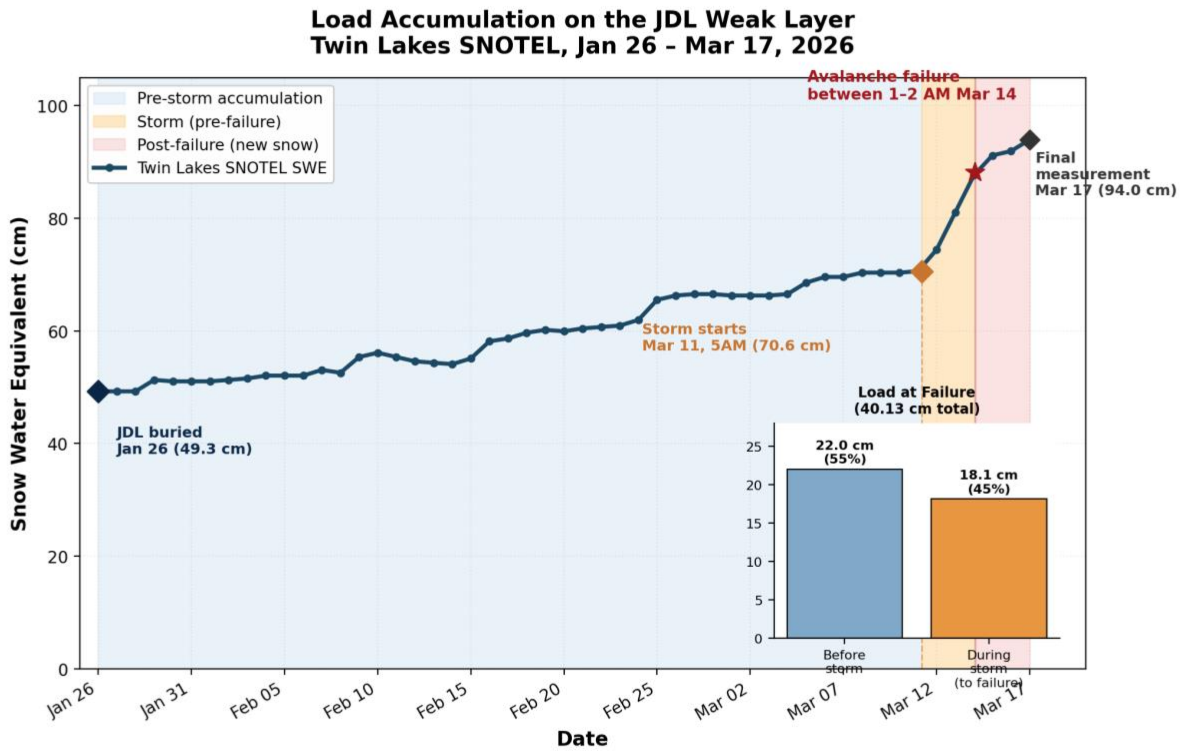

Figure 2: Twin Lakes SNOTEL SWE record, Jan 26 – Mar 17, 2026, showing load accumulation on the JDL weak layer, with storm start, estimated failure time, and final measurement marked. Inset: pre-storm vs. storm contribution to the 40.13 cm (15.8 in) failure load.

4.2 Method validity

The core assumption of this study is the proportional SWE accumulation between the crown site and the Twin Lakes SNOTEL site despite the 6.5 km (4 mi) separation and 370 m (1,200 ft) elevation difference. This study did not have a strong way to verify this assumption, as there is limited data in the region and there was no way to observe the storm in real time. If the proportionality assumption was off by 5 percentage points, the shift in timing would be 7 hours, and still add more precision than avalanche warnings by the forecast team.

4.3 Aspect spatial patterns

The sampling of avalanche crown data provided valuable insights into the sensitivity distribution of the JDL and the wind loading patterns of the overloading storm. The weighted vs unweighted R values illustrate 2 key points for the avalanche distribution. Comparing the weighted and unweighted results allowed us to evaluate whether larger avalanches were aligned with the dominant wind-loading direction than smaller ones. The mass-weighted R value of 0.92 illustrates the effects of wind within a storm as a method of snow transportation and loading. Forecasted and modeled strong winds from the WSW throughout the duration of the storm led to primary loading of NE aspects where the largest avalanches occurred. While the unweighted R value of 0.882 still shows a strong correlation with wind loading patterns, it also illustrates the more sensitive nature of the JDL weak layer on shaded aspects. The outlier avalanches occurred on NW aspects that experience some wind loading, but not significant amounts according to the images. No deep persistent avalanches on solar aspects were reported during this storm.

4.4 Elevation distribution patterns

The sampling of avalanche crown data made it easy to evaluate elevation as a factor in this avalanche cycle. The weighted and unweighted distributions showed a majority (62% and 54%) of avalanches occurred between 2,210 and 2,362 m (7,250 and 7,750 ft), which is consistent with strong winds depositing snow downslope of peaks and ridgelines. This aligns with the wind patterns of the storm, where sustained winds of 48–64 km/h (30-40 mph) with gusts into the 97 km/h (60 mph) range likely transported snow long distances, past areas of typical wind loading patterns. In addition, there are significantly less high elevation areas in the study area, so proportionally there are less avalanches. The lowest elevations sampled have denser tree cover which have a large influence on the likelihood of deep slab avalanches. Lower elevations that did slide were in areas with little tree cover.

4.5 Limitations

This study has several limitations that should be considered when interpreting the results, two of which we view as the most significant constraints on this work: the single avalanche cycle scope of this case study, and the reliance on photo-based crown mapping.

This case study only examines one avalanche cycle, triggered by one storm, on one known weak layer in one small region. The loading analysis itself does draw on the full season and several storms leading up to that trigger, but the avalanche cycle we are explaining is still a single event. There is not enough data to confidently say the pre-storm vs storm load amounts, the dominance of wind loading, or the elevation banding are definitive of deep slabs in general, or are specific to this weak layer, this season's storm sequence, and this terrain. Applying this same hindcasting/field study method to additional avalanche cycles and weak layers will help determine if these patterns exist across different events, seasons, terrain, and weak layers. This is the most valuable direction for future work stemming from this study.

The crown mapping relied on human interpretation of Ben's photos, compared against 3D terrain models and aerial imagery to map each crown onto terrain features. This process introduced the potential for georeferencing error, as the crown mapping is inherently a visual estimate, and error in this process could tweak individual crowns' aspects or elevations by a small percentage. Additionally, crowns were observed, but only one crown was visited and sampled, so this study assumes all the observed avalanches occurred on the JDL and occurred around a similar time. This study also relied on a single SNOTEL station as the proxy for loading across the entire study area, despite known spatial variability in wind and precipitation across the terrain.

5. CONCLUSIONS

We found that it took a large amount of SWE, almost as much as it had been supporting, to overload the JDL. We also found that the accumulation rates at the crown wall study site were similar enough to those at the Twin Lakes SNOTEL to use a proportionality calculation to pinpoint failure timing. This method placed the avalanche's occurrence in the early morning of March 14th, consistent with the forecasting team's field-based timeline.

The crown mapping data indicated that most avalanches occurred in both shaded aspects and wind loaded areas, and therefore wind loading was likely a key factor in overloading the weak layer, both in where avalanches occurred and how quickly the layer was pushed toward failure.

This data could be used in a practical situation to help predict failure timing during future similar storms in the area. This case study shows that a small forecasting team with limited resources can still produce meaningful, data-driven insight into a storm cycle after the fact, using tools that are already available to them: SNOTEL data, field sampling, and photo-based crown mapping.

6. FUTURE WORK

This is a single case study, so the patterns identified here should be tested further before being treated as general rules. A few directions could help with that.

Collecting data from more case studies like this one would build a larger dataset and help determine if these patterns hold up across different storms, weak layers, and terrain, or if this storm was a unique case.

Running this same study in an area with more weather and snowfall collection stations would also help. This study relied on a single SNOTEL station as a proxy for loading across the whole study area, and having multiple stations to compare against would help verify the proportionality assumption this method depends on.

Finally, running this same hindcast approach in an area with camera or sensor coverage could let the SWE proportionality method be validated against a known, observed failure time, rather than just a forecaster's field-based timing window like the one used here.

ACKNOWLEDGEMENTS

Thank you to the Natural Resources Conservation Service (NRCS) for maintaining the Twin Lakes SNOTEL station and providing the data that made this study possible. Thank you to Leah Nuese-Yaker for her help editing and developing ideas throughout this project. Thank you to Silver Mountain Resort for loaning field equipment.

REFERENCES

LaChapelle, E.R., 1980. The fundamental processes in conventional avalanche forecasting, J. Glaciol., 26(94), 75–84.

Mock, C.J., Birkeland, K.W., 2000. Snow avalanche climatology of the western United States mountain ranges, Bull. Am. Meteorol. Soc., 81(10), 2367–2392.

Natural Resources Conservation Service (NRCS), 2026. Twin Lakes (836) SNOTEL Site Information and 1991–2020 Normals. USDA National Water and Climate Center. Available at: https://wcc.sc.egov.usda.gov/nwcc/site?sitenum=836 (accessed August 2026).

Schauer, A., Moderow, A., Johnston-Bloom, A., 2024. Meteorological and snowpack properties associated with crust-adjacent persistent weak layers, part 2: Applying theory to observed patterns, in: Proceedings of the International Snow Science Workshop, Tromsø, Norway, [pg 163].